# Evidence for an Oxygen Diffusion Model for the Electric Pulse Induced Resistance Change Effect in Transition-Metal Oxides

Y. B. Nian, J. Strozier, N. J. Wu, X. Chen, and A. Ignatiev
*Center for Advanced Materials, University of Houston, Houston, Texas, 77204-5004, USA*
(Received 21 January 2006; published 4 April 2007)

Electric-pulse induced resistance hysteresis switching loops for $Pr_{0.7}Ca_{0.3}MnO_3$ perovskite oxide films were found to exhibit an additional sharp ''shuttle tail'' peak around the negative pulse maximum for films deposited in an oxygen-deficient ambient. The resistance relaxation in time of this ''shuttle tail'' peak as well as resistance relaxation in the transition regions of the resistance hysteresis loop show evidence of oxygen diffusion under electric pulsing, and support a proposed oxygen diffusion model with oxygen vacancy pileup at the metal electrode interface region as the active process for the nonvolatile resistance switching effect in transition-metal oxides.

DOI: 10.1103/PhysRevLett.98.146403 PACS numbers: 71.30.+h, 73.40.−c, 73.50.−h

Driven by an increasing demand for nonvolatile memory, a novel electrical pulse induced resistance change effect (EPIR) [1] observed in transition-metal oxide layers including perovskite oxides ReAMO (Re, rare-earth ions; A, alkaline ions; M, transition-metal ions) has attracted extensive interest [2–6]. Under EPIR, the resistance of a metal-oxide-metal thin film device can be dramatically and repeatedly switched between a high and a low value by applying electric pulses with opposite polarities over a wide temperature range, and without any applied magnetic field. This reversible *R*-switching effect has been found to take place in a very large number of insulating oxide systems, ranging from simple binary oxides, to the more complex three, four, and five-component perovskites, including manganites [1], zirconates [2], cuprates [5], and titanates [6].

The underlying physics of the EPIR effect, however, is not yet well known. Models proposed include charge trapping or detrapping [7], Schottky barrier behavior at the metallic contact interface [8], conducting filament creation or destruction [6], and creation of crystalline defects by the applied electric field [9].

All of the models leave unanswered questions. The Schottky barrier model is not likely since the EPIR effect has been clearly observed in many $M1$-oxide-$M2$ sandwich device structures, including *n*-type and *p*-type oxides and different metallic electrode ($M1/M2$) with higher or lower work functions. Trap centers have not been identified for resistive switching, nor do they address long-term retention. Although filaments have been observed in insulating oxide films with very high average resistivity [6], most conducting filamentary paths formed by a pulse of one polarity cannot be generally destroyed by application of an electric pulse with the opposite polarity. Similar arguments occur for the defect models.

We report here an oxygen vacancy diffusion mechanism based on the observation of resistance relaxation with time and temperature in the voltage switching region of a PCMO-based EPIR device, and based on activation energy measurements, we conclude that oxygen vacancies and their motion play the driving role in the EPIR phenomenon.

Conduction in $Pr_{0.7}Ca_{0.3}MnO_3$ (PCMO) at room temperature is thought to occur by hopping of carriers consisting of small polarons along -Mn—O—Mn—O— chains and/or by percolation through ferromagnetic droplets in a paramagnet insulating matrix [10,11]. In either case, the process is thermally activated with an activation energy of about 100–200 meV where the character of the conduction is thought to be holes. The absence of oxygen atoms (or the presence of oxygen vacancies) in a -Mn—O—Mn—O— chain is assumed to disrupt the conduction process with the vacancies acting as strong scatterers for the ''hole'' polarons. Indeed, the resistivity of $ReAMnO_{3-x}$, such as $LaBaMnO_3$, has been reported to increase by more than 4 orders of magnitude at room temperature when the oxygen content is reduced by ~5% [12]. Further, it is often the case that the surface region of an oxide is oxygen deficient compared to the bulk, containing perhaps 5% or more oxygen vacancies in the surface region [13]. Electrodes evaporated or sputtered onto an oxide sample will be in contact with this oxygen-deficient surface region, and hence the sample should show high resistivity. This is generally seen in PCMO metal-oxide-metal devices where measured resistance between electrodes deposited on PCMO is much larger than what one would expect from the bulk resistivity of PCMO ($10^{-1}$ to $10^{-2}$ Ω cm for bulk [14] vs $10^3$ to $10^4$ Ω cm for thin film [1,4]). It is well to note here that the samples described here are asymmetric thin film devices as the resistance of the device comes principally from the interface region between the perovskite oxide surface and the top metal electrode. As a result, we have focused this study on the oxygen-deficient growth of thin film PCMO for the investigation of resistance switching mechanisms in oxides.

Figure 1(a) shows the device structure and measurement setup used in this study. $Pr_{0.7}Ca_{0.3}MnO_3$ films were grown by rf sputtering on bottom electrode (BE) Pt films deposited on $TiN/SiO_2/Si$ substrates. The PCMO films were

 

grown at 500 °C under 60 mTorr ambient gas which was either oxygen rich (argon:oxygen = 2:1), or oxygen-deficient (Ar only). 300 $\mu$m diameter Ag top electrode (TE) pads were deposited onto the PCMO films by dc sputtering for subsequent resistivity measurements. The PCMO films were ~400 nm thick with a surface roughness <10 nm. Resistance switching of the samples was investigated by applying electrical pulses of up to ±5 V across the top Ag electrode and bottom Pt electrode, and the resistance was measured by applying a 1 $\mu$A dc current and reading the corresponding voltage across the film after each applied electric pulse. A positive pulse applied to the sample is defined as current passing into the PCMO film through the TE and out from the BE, and a negative pulse is applied in the reversed direction.

Resistance hysteresis switching loops (HSL) were measured by applying a sequence of pulses with a constant voltage step. Increasing negative pulses were applied when the sample was in its low resistance state until the sample reached a high resistance state. The pulse magnitude was then reduced until a change of polarity to positive after which the positive pulses were increased in magnitude until the sample switched to the low resistance state. Figure 1(b) shows the HSL of a standard sample grown by rf sputtering in a standard argon/oxygen (2:1) mixed ambient gas. The high resistance state, identified as region HSL-I, and the low resistance state, identified as region HSL-III, are the EPIR bistates, and the regions HSL-II and HSL-IV are the resistance transition regions of the EPIR device. Samples grown in an oxygen-deficient atmosphere [Fig. 1(c)] were found to have a sample initial resistance that was much higher than that of a standard sample [Fig. 1(b)], as expected, due to an increase in vacancies. Moreover, the hysteresis loop for the oxygen-deficient sample shows an unexpected rise to very high resistance values (above the stable high resistance state) under negative pulsing, which then reduces to the high resistant state as the negative pulsing voltage is decreased thus producing a "shuttle tail" peak in the hysteresis loop [the regions HSL-V and HSL-VI in Fig. 1(c)]. This "peak" was found to dramatically decay in time as shown in Fig. 2.

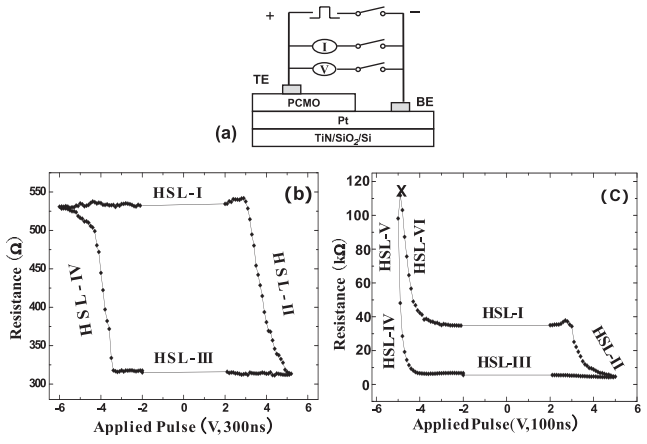


FIG. 1. Resistance HSL for PCMO EPIR devices: (a) EPIR device structure and electrical measurement setup; (b) HSL for a PCMO film grown in an oxygen environment; (c) HSL for a PCMO film grown in an oxygen-free environment (X: the point at which resistance relaxation was measured).

To understand the origin of this shuttle tail and its resistance decay behavior, we have carefully looked at the dynamic response of all sections of the hysteresis switching loop. The resistance as a function of time was measured after each voltage pulse was applied until the resistance reached its stabilized value. It was found that in the shuttle tail regions (HSL-V&VI) and the transition regions (HSL-II&IV) of Fig. 1(c), the resistance relaxed back towards the value before the switching pulse was applied as seen in Figs. 2 and 3; i.e., the resistance relaxation is always opposite to the resistance change resulting from the switching pulse. What is interesting is that the relaxation process reported here takes place only in the "tail" and transition regions, where the switching process also occurs. The stable ($>10^8$ sec) resistance states, $R_H$ in HSL-I and $R_L$ in HSL-III, showed no relaxation except where they border the transition region (Fig. 3). These results imply that once the forcing function to the out-of-equilibrium state (negative or positive pulses) is removed, the system moves by diffusion of the active species toward the stable (low or high) resistance state.

Since we have discussed that oxygen vacancies in oxides cause resistance change, we propose here a switching model for the EPIR effect which incorporates oxygen ion/vacancy motion, whereby a positive pulse of sufficient magnitude and duration will move oxygen ions into vacancies located near the metal electrode interface thus patching otherwise broken chains of -Mn—O—Mn—O—, and thereby decreasing the resistance. A sufficient negative pulse will have the opposite effect, moving oxygen vacancies into the interface region, and piling them up at the metal interface, thereby breaking the -Mn—O—Mn—O— chains and increasing the resistance. The oxygen ion-vacancy concentration can be locally overdriven at the metal interface leading to a nonequilibrium ion (va-

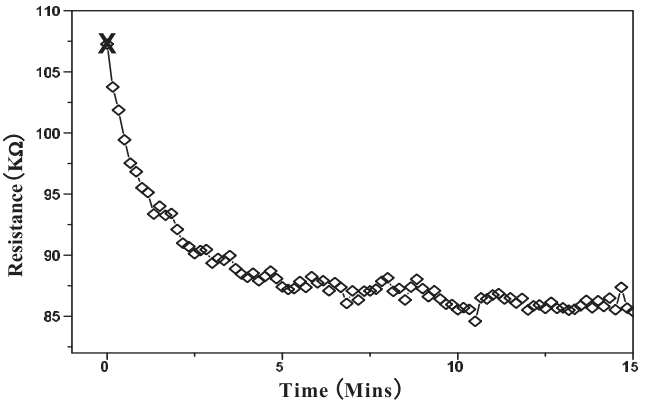


FIG. 2. Time decay of the resistance at the peak of the shuttle tail [X point in Fig. 1(c)] in the HSL ($T$ = 300 K).

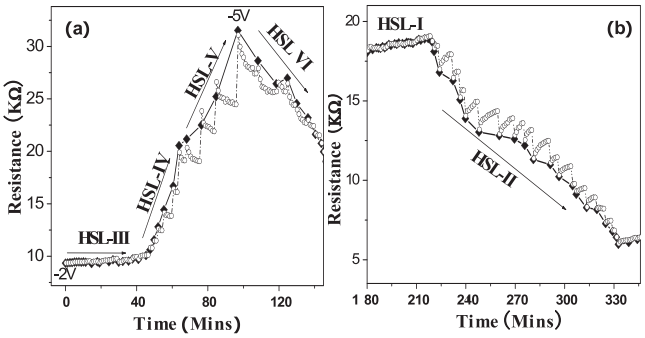


FIG. 3. Resistance relaxation (circle) opposite to the direction of resistance change upon pulsing (black diamond) for the transition region of the HSL: (a) resistance decreases after negative pulse; (b) resistance increases after positive pulse.

cancy) distribution that undergoes relaxation, e.g., the shuttle tail peak decay with time. The measured dynamic current density during switching is $\sim 10^1$ to $10^2$ amps/cm$^2$ (Fig. 4), and hence may play a critical role in oxygen or vacancy movement in the interface region of the sample as enhanced oxygen diffusion in oxides under high current densities has been reported [15]. Thus in our model, the high dynamic current density during pulse induced switching enhances oxygen mobility, while the pulse polarity drives the mobile ions toward/away from the electrode interface region.

Although oxygen motion in EPIR has been mentioned in several papers [3,5,6], to the best of our knowledge, no convincing evidence has been provided to support oxygen diffusion in an EPIR device and its relationship to resistance switching. To corroborate our proposed oxygen/vacancy diffusion mechanism, we modeled vacancy concentration by a half-Gaussian, with the peak equal to maximum concentration of oxygen vacancies in PCMO at the metal electrode interface, and the width given by the thickness of the active region. The solution of the one-dimensional diffusion equation for the oxygen concentration initial condition can be written in closed form [16]:

$$C(x,t) = C(0,0)L\frac{\exp[-x^2/(4L^2/4 + Dt)]}{2(L^2/4 + Dt)^{1/2}}. \quad (1)$$

Here $C(0,0)$ is the initial oxygen vacancy concentration value, $D$ is the diffusion constant with $D = D_0 \exp(-E/kT)$, $L$ is the width of the initial concentration (we take the thickness of the active layer to be $4L$), and $t$ is the decay time.

We further define $R_{\text{peak}}$ as the maximum resistance at the shuttle peak, $R_H$ as the stable high resistance state (HSL-I). Since the resistivity of a similar perovskite oxide ($La_{0.67}Ba_{0.33}MnO_3$) shows an exponential relationship with oxygen vacancies at room temperature [12], we assume the resistivity of PCMO also has an exponential relationship with oxygen vacancy concentration. However, it is expected that vacancy changes of less than 5% are active under electric-pulse switching. As a result, we take a linear expansion of the exponential concentration dependence to yield resistivity in the active region of the PCMO sample proportional to the oxygen vacancy concentration plus a constant. Note that the $R_{\text{peak}}$ is proposed to be due to the nonequilibrium concentration. We can factor out $C(0,0)$ and the change in resistivity per oxygen vacancy by introducing the function $Z(t)$:

$$Z(t) = \left(\frac{R_{\text{peak}} - R_H}{R(t) - R_H}\right)^2 = 1 + 4\frac{D}{L^2}t \quad (2)$$

Since $Z(t)$ is defined as a function of experimental parameters only, and plots of $Z(t)$ vs time for a given temperature, $T$, should yield a straight line with a slope of $4D(T)/L^2$. The resistance decay of the shuttle tail peak at different temperatures was measured, with $Z(t)$ vs $t$ shown in Fig. 5(a). Within considerable noise of the data, the curves approximate straight lines as predicted in Eq. (2). Plotting ln[slope$Z(t)$] against $1/T$ in Fig. 5(b) yields a slope $E/k = 4550$ K, resulting in an activation energy for diffusion of about 0.4 eV.

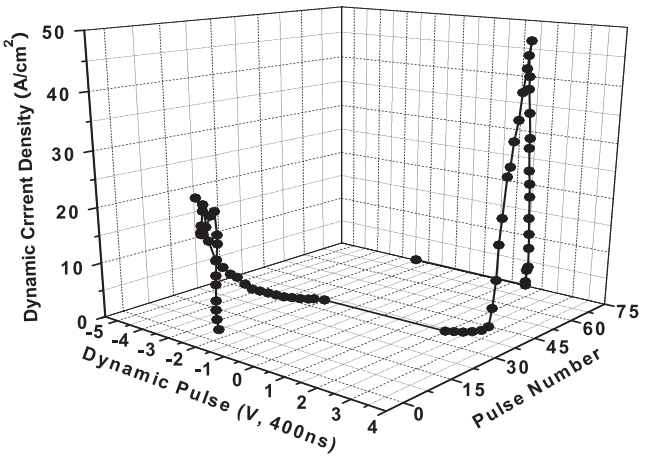


FIG. 4. Dynamic current density as a function of pulse voltage around the dynamic hysteresis switching loop.

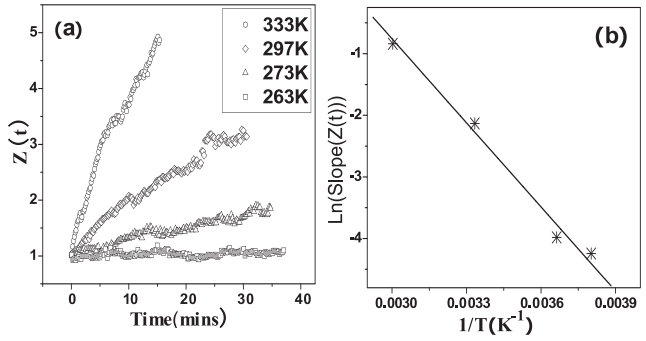


FIG. 5. (a) $Z(t)$ at different temperatures (333 K, 297 K, 273 K, 263 K); (b) Natural log of the slope in (a) vs $1/T$ with a linear fit [slope in (b): $-4500$ K].

Gramm *et al.* [17] have measured the oxygen diffusion constant at room temperature in the perovskite oxide $Bi_2Sr_2CaCu_2O_{8+d}$ as $1.6 \times 10^{-17}$ $cm^2\,sec^{-1}$, with an activation energy of about 0.6 eV and $D_0$ about $2 \times 10^{-7}$ $cm^2\,sec^{-1}$. From our $Z(t)$ data and assuming diffusion length of ~100 nm as has been recently observed by I-AFM measurements [18]; we calculate the oxygen diffusion constant to be about $5 \times 10^{-14}$ $cm^2\,sec^{-1}$ at room temperature, and $D_0$ about $2.6 \times 10^{-7}$ $cm^2\,sec^{-1}$. This prefactor is very close to the value reported by Gramm *et al.*, indicating similar ionic size and similar attempt frequencies of the diffusing species in our PCMO samples, i.e., oxygen ions.

The above data point to the following description of the PCMO resistance hysteresis switching loop behavior. In order to support the original PCMO lattice, there is a maximum value for local oxygen vacancy concentration that we call $O_{v\,\max}$. For values less than $O_{v\,\max}$, oxygen diffusion in PCMO remains at the very low thermal equilibrium value quoted in the literature for like-structured oxides, and such diffusion yields the time constant controlling the long resistance state persistency, $t_p > 10^8$ sec of the EPIR effect. For oxygen vacancy concentrations greater than $O_{v\,\max}$, the local lattice becomes distorted and strained, leading to a greatly increased diffusion constant for oxygen, such as measured here, which brings the relaxation time constant $t_r$, to the order of minutes. The vacancy concentration is increased by the electric-pulse switching process which is so fast ($t_s = 10^{-7}$ s) that each pulse leaves the system in a state of temporary nonequilibrium, even in the nontail transition region, and the system simply relaxes back from this high concentration state via the more rapid strain enhanced oxygen diffusion process reported here.

The complete mechanism of the EPIR effect might, however, be more complicated due to the strong coupling between electronic, spin, orbital, and elastic degrees of freedom in these complex oxides. Oxygen vacancies in the lattice would increase the $Mn^{3+}/Mn^{4+}$ ratio, thus increasing the average Mn ionic size. Such lattice distortion with increasing lattice parameters would engender structural fluctuations and increase the probability of oxygen diffusion. The possible presence of inhomogeneous phases with nanometer and/or micrometer scales [10] may also affect oxygen ion (vacancy) motion in perovskite oxides further enhancing the EPIR effect.

This oxygen diffusion model can be well applied to other oxide systems, which show the EPIR effect including those with filamentary behavior. Further advancement of the vacancy diffusion model will require overcoming the difficulties of direct measurement of vacancy concentration at the nanometer scale.

In summary, we propose a model for the EPIR effect in perovskite oxide thin films where we have shown oxygen ions (vacancies) are the active agents for the nonvolatile EPIR switching effect in PCMO. The model we propose for resistance switching in EPIR incorporates enhanced mobility of oxygen ions (vacancies) and resultant pileup of these species near the metal electrodes under large current injection during a switching pulse. This results in a local change of concentration of oxygen ions (vacancies) near the electrodes thereby changing the resistance. Although the model and relevant discussions here are mostly based on transition-metal perovskite oxide, they can fit the electric-pulse induced resistance switching in binary transition-metal oxides and other complex oxides as well.

Assistance is acknowledged from Mickael Maman and Dr. Christina Papagianni. Partial support for this work is acknowledged from NASA, Sharp Laboratories of America, the State of Texas, through the Center for Advanced Materials, and the R. A. Welch Foundation.

[1] S. Q. Liu, N. J. Wu, and A. Ignatiev, Appl. Phys. Lett. **76**, 2749 (2000).
[2] A. Beck, J. G. Bednorz, C. Gerber, C. Rossel, and D. Widmer, Appl. Phys. Lett. **77**, 139 (2000).
[3] A. Baikalov, Y. Q. Wang, B. Shen, B. Lorenz, S. Tsui, Y. Y. Sun, Y. Y. Xue, and C. W. Chu, Appl. Phys. Lett. **83**, 957 (2003).
[4] A. Sawa, T. Fujii, M. Kawasaki, and Y. Tokura, Appl. Phys. Lett. **85**, 4073 (2004).
[5] N. A. Tulina, A. M. Ionov, and A. N. Chaika, Physica (Amsterdam) **C366**, 23 (2001).
[6] K. Szot, W. Speier, G. Bihlmayer, and R. Waser, Nat. Mater. **5**, 312 (2006).
[7] M. J. Rozenberg, I. H. Inoue, and M. J. Sanchez, Phys. Rev. Lett. **92**, 178302 (2004).
[8] T. Fujii, M. Kawasaki, A. Sawa, H. Akoh, Y. Kawazoe, and Y. Tokura, Appl. Phys. Lett. **86**, 012107 (2005).
[9] S. Tsui, Y. Q. Wang, Y. Y. Xue, and C. W. Chu, Appl. Phys. Lett. **89**, 123502 (2006).
[10] E. Dagotto, T. Hotta, and A. Moreo, Phys. Rep. **344**, 1 (2001).
[11] M. B. Salamon and M. Jaime, Rev. Mod. Phys. **73**, 583 (2001).
[12] H. L. Ju, J. Gopalakrishnan, J. L. Peng, Li Qi, G. C. Xiong, T. Venkatesan, and R. L. Greene, Phys. Rev. B **51**, 6143 (1995).
[13] F. Chen, T. Zhao, Y. Y. Fei, H. Lu, Z. Chen, G. Yang, and X. D. Zhu, Appl. Phys. Lett. **80**, 2889 (2002).
[14] Y. Tomioka, A. Asamitsu, H. Kuwahara, Y. Moritomo, and Y. Tokura, Phys. Rev. B **53**, R1689 (1996).
[15] S. H. Huerth, H. D. Hallen, and B. Moeckly, Phys. Rev. B **67**, 180506 (2003).
[16] M. E. Glicksman, *Diffusion in Solids: Field theory, Solid-State Principles, and Applications* (Wiley, New York, 2000).
[17] A. Gramm, Th. Zahner, U. Spreitzer, R. Rossler, J. D. Pedarnig, D. Bauerle, and H. Lengfellner, Europhys. Lett. **49**, 501 (2000).
[18] X. Chen, N. J. Wu, J. Strozier, and A. Ignatiev, Appl. Phys. Lett. **89**, 063507 (2006).